EXPERIMENTAL INVESTIGATIONS OF GENERALIZED PREDICTIVE CONTROL FOR TILTROTOR STABILITY AUGMENTATION

Mark W. Nixon[1], Chester W. Langston[2], Jeffrey D. Singleton[3], David J. Piatak[4], Raymond G. Kvaternik[5], Richard L. Bennett[6], and Ross K. Brown[7]

[1,2,3]U.S. Army Research Laboratory, NASA Langley Research Center
M.S. 340, Hampton, Virginia 23681, USA
email: m.w.nixon@larc.nasa.gov, c.w.langston@larc.nasa.gov, j.d.singleton@larc.nasa.gov

[4,5]Aeroelasticity Branch, NASA Langley Research Center
M.S. 340, Hampton, Virginia 23681, USA
email: d.j.piatak@larc.nasa.gov, r.g.kvaternik@larc.nasa.gov

[6,7]Bell Helicopter Textron, Inc.
PO BOX 482, Fort Worth, Texas 76101, USA
email: dbennett@bellhelicopter.textron.com, rbrown2@bellhelicopter.textron.com

Key words: Active Control, Stability Augmentation, Tiltrotor, Soft-Inplane

Abstract. A team of researchers from the Army Research Laboratory, NASA Langley Research Center (LaRC), and Bell Helicopter-Textron, Inc. have completed hover-cell and wind-tunnel testing of a 1/5-size aeroelastically-scaled tiltrotor model using a new active control system for stability augmentation. The active system is based on a generalized predictive control (GPC) algorithm originally developed at NASA LaRC in 1997 for unknown disturbance rejection. Results of these investigations show that GPC combined with an active swashplate can significantly augment the damping and stability of tiltrotors in both hover and high-speed flight.

1 INTRODUCTION

1.1 Stiff-inplane versus soft-inplane rotor systems for tiltrotors

While three-bladed, gimballed, stiff-inplane rotor systems are employed for the current generation of tiltrotors (XV-15, V-22, BA609), the weight and performance penalties of stiff-inplane rotors may become too significant for use on systems larger than the V-22. When operating in airplane mode, rotor loads are usually small compared to those experienced when operating in helicopter mode. This is due to reduced disk loading and axisymmetric inflow conditions in airplane mode. However, during airplane-mode maneuvers such as a rapid pull-up, high oscillatory inplane rotor loads are developed. Tiltrotors employ large highly-twisted blades, creating a significant aerodynamic forcing in the inplane direction where the centrifugal restoring forces are much lower than those associated with the flapping direction. Stiff-inplane hubs must be designed to accommodate these inplane loads using additional structure, which increases weight and can make the inplane stiffness higher still, leading to more increases in the inplane loads. For larger tiltrotors, this cyclic design challenge can lead to very high structural weights or even to an infeasible design altogether. As a design trade-off, the maximum aerodynamic load capability of a large tiltrotor may be limited to reduce the structural weight of the

Presented at the 2001 CEAS / AIAA / AIAE International Forum of Aeroelasticity and Structural Dynamics, Madrid, Spain, June 5-7, 2001.

hub. Such is the case for the V-22 which currently employs a controller to limit the body pitch-rate motion of the aircraft and thereby curtail rotor inplane loads which could otherwise rise above their design allowables (Ref. 1).

Soft-inplane rotor systems can significantly reduce the inplane rotor loads generated during maneuvers of larger tiltrotors, thereby reducing strength requirements on the hub, leading to reduced structural weight and improved aircraft agility. For a soft-inplane rotor system to be effective, it should have a lag mode* frequency below about 0.9/rev, otherwise the loads are about the same as those of the stiff inplane rotor system. While there are significant benefits for soft-inplane rotor systems with respect to loads and weight, these rotor systems have two major shortcomings with respect to their stiff-inplane counterparts. First, in high-speed flight they tend to have lower whirl-flutter stability boundaries, and second, in hover they are subject to instabilities associated with ground resonance. Before soft-inplane rotor systems become viable for application to tiltrotors, new techniques must be developed to augment the stability of these rotor systems in both the hover and the high-speed flight regimes.

1.2 Ground resonance considerations

Ground resonance instability is only a concern for soft-inplane rotor systems, and is not a consideration for the current generation of stiff-inplane tiltrotors. To date, the most significant studies of tiltrotor systems subject to ground resonance conditions were made by Boeing Helicopter with the development of their Model 222 tiltrotor concept, a hingeless soft-inplane rotor system, which was their entry into a NASA/Army-sponsored tiltrotor research aircraft program (eventually named the XV-15). Ground and air resonance behavior of the Boeing soft-inplane configuration was addressed in several experimental and analytical studies using different size rotor test apparatuses, beginning with a 1/10-scale wind-tunnel model as described in Ref. 2, and ending with a full-scale 26-ft. diameter semispan model tested in the NASA Ames 40- x 80-ft. tunnel as described in Refs. 3 and 4. The Boeing soft-inplane design had a relatively high inplane natural frequency, such that the design rotor speed in hover mode did not create a ground resonance problem. Experimental results were obtained for this configuration with the system in airplane mode subject to air resonance conditions, and those results are very similar to a ground resonance type instability. This configuration was also not gimballed; it was a typical hingeless soft-inplane design. Thus, the tiltrotor configuration of the current study is unique in two important design parameters: 1) the use of a gimbal and constant velocity joint which has a significant effect on the Coriolis forces, and 2) the use of a "low" lag frequency (about 0.5/rev) which creates a resonance condition between the low-frequency lag mode and the critical tiltrotor pylon/wing mode that is well within the design rotor speed envelope.

1.3 Proprotor whirl-flutter considerations

Proprotor whirl-flutter is an aeroelastic instability encountered by tiltrotors at high speeds in airplane mode, and it is a primary consideration in the design of tiltrotor aircraft. Because wing torsional stiffness is the major design parameter influencing this instability, the stability requirements of current tiltrotor aircraft (XV-15, V-22, BA-609) have been attained by using thick, torsionally stiff wings having a 23% thickness-to-chord ratio. Such

*The term "lag mode" will be used throughout the remainder of the paper as a description of the rotor lead-lag mode; however, the terms "inplane" and "lag" will be used interchangeably to be consistent with common usage of the industry.

wings provide the torsional stiffness required for stability in those aircraft, albeit at the expense of cruise efficiency and maximum speed. The use of thinner wings would permit higher cruise speeds, increased range, and improved productivity. However, the attendant reduction in wing stiffness would bring with it the problem of proprotor whirl-flutter instability. Thus, aeroelastic instability of the proprotor/pylon/wing system stands as the primary barrier to increasing the maximum speed capability of tiltrotor aircraft. Also, as mentioned in the previous section, a soft-inplane rotor system will generally encounter whirl-flutter at lower speeds than its stiff-inplane counterpart, so there is additional effort associated with expanding the stability envelope for soft-inplane rotor systems in high-speed cruise.

1.4 Previous studies of active control for tiltrotor stability augmentation

While both passive and active means for augmenting tiltrotor stability have been studied, the current paper will focus only on the active control concepts. There have been a number of studies dealing with the use of active controls for improving the aeroelastic behavior of tiltrotor aircraft. However, most of these have addressed the problem of gust and maneuver load alleviation, and there has been only limited attention given to the use of active controls for stability augmentation (Refs. 5-8). Ref. 5 investigated the application of swashplate feedback for augmentation of aeroelastic stability as part of a broader study of feedback control for improving the aeroelastic and rigid-body flight characteristics of soft-inplane tiltrotor aircraft. The baseline configuration of those studies was the Boeing Model 222. Bode analyses were used to define the appropriate gains and phases to be applied to the wing responses that were to be fed back to the swashplate cyclic inputs. Refs. 6-7 were analytical studies of feedback control for increasing proprotor/pylon stability on an XV-15 size tiltrotor aircraft. A feedback gain matrix was introduced into the formulation by adding a feedback loop to the equations of motion linearized about a flight condition of interest. Wing tip vertical velocities and accelerations were used for feedback. The gains needed to stabilize the system were determined by simply varying the terms in the gain matrix until an eigenvalue analysis of the closed-loop system indicated a stable system. Ref. 8 was an analytical study into the use of linear quadratic regulator techniques for determining the wing feedback gains needed to stabilize the whirl modes of a tiltrotor aircraft using an active swashplate. The method was studied using a mathematical model that had been developed earlier for a full-size semi-span configuration of the XV-15. Control design was done in modal space.

The studies described in the previous paragraph show that active methods for tiltrotor stability augmentation are a less-than-mature subject area. Most studies have been formulated only through analysis, and those that have included an experimental investigation have used a trial-and-error approach for determination of the control inputs that produce a stable system. There remains a need for extended development of active control methodologies, both analytical and experimental, that may be more applicable for development of production tiltrotor systems.

1.5 Current experimental investigations of active stability augmentation

A team of researchers from the Army Research Laboratory (ARL), NASA Langley Research Center (LaRC), and Bell Helicopter-Textron, Inc.(BHTI) have completed two experimental investigations of active stability augmentation on the Wing and Rotor Aeroelastic Testing System (WRATS), a 1/5-size aeroelastic semi-span model based on the V-22. The active control system employed for both studies consisted of a gener-

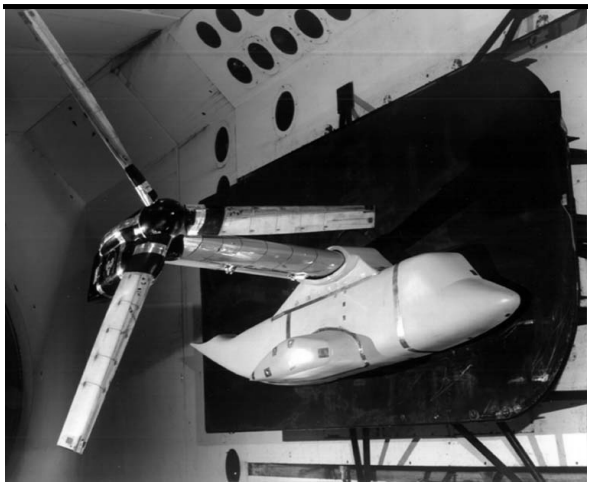

Figure 1: WRATS in the TDT.

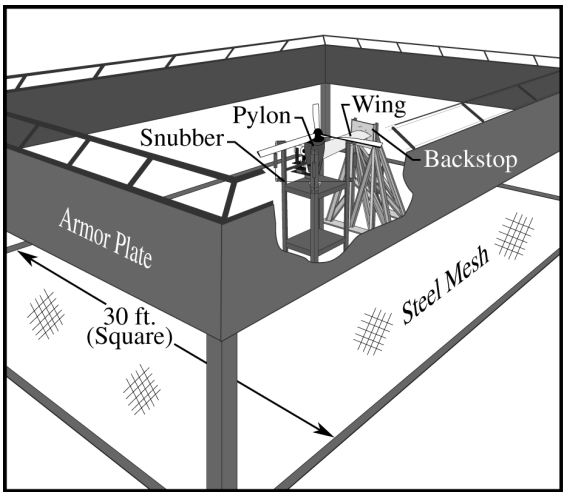

Figure 2: WRATS in the hover cell.

alized predictive control (GPC) algorithm, a real-time digital processor, and a set of 3 high-frequency actuators in the pylon, which position the swashplate according to both the pilot control commands (DC signals) and the active control commands (AC signals). The investigations have considered a soft-inplane gimballed hub subject to ground resonance conditions in hover (October 1999), and a stiff-inplane gimballed hub subject to whirl-flutter conditions in airplane mode (April 2000). These efforts were planned as part of a Memorandum of Agreement between NASA LaRC and BHTI to "Perform Experimental Aeroelastic Studies of a Tiltrotor Model," and represent the first two experimental investigations related to GPC stability augmentation in a planned series of tests to be conducted at the Transonic Dynamics Tunnel (TDT). These investigations show significant improvements in damping of critical modes of the WRATS model in both hover and high-speed cruise, lending promise for further development of the GPC active stability augmentation system. The purpose of this paper is to document the significant improvements in damping, and the associated augmentation of stability, that may be obtained using GPC on a tiltrotor configuration in two very different flight regimes.

2 APPARATUS

The experimental studies were performed in two locations: the wind-tunnel testing was conducted in the TDT at the NASA Langley Research Center in Hampton, Virginia (Fig. 1), and the hover testing was performed in the WRATS 30' x 30' hover cell (Fig. 2) located in a high-bay building adjacent to the TDT. The TDT is a continuous flow, single return, variable pressure tunnel having a test section 16-feet square with cropped corners. The control room and test section walls are provided with large windows for close viewing of the model. The tunnel is capable of operation at stagnation pressures from near vacuum to slightly above atmospheric and at Mach numbers from near zero up to about 1.2. Either air or a heavy gas (R-134a) can be used as the test medium. Both the density and test-section Mach number are continuously controllable. The present wind-tunnel investigation was conducted in air under near atmospheric conditions and at free-stream Mach numbers less that 0.30.

Notable features of the WRATS hover facility are a backstop mount which centers the tiltrotor model in the hover cell with wing root mounted 8 ft. above the floor (same as when mounted in the TDT wind-tunnel test section); a snubber stand to halt pylon motion in the event of an instability; a 3000 psi hydraulic system; a 100 psi air supply; a 440 volt

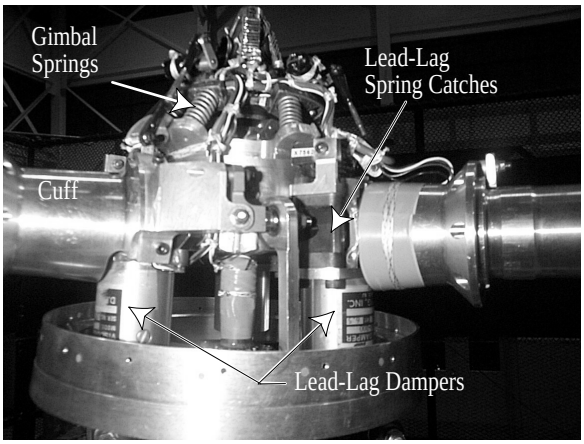

Figure 3: Soft-inplane hub.

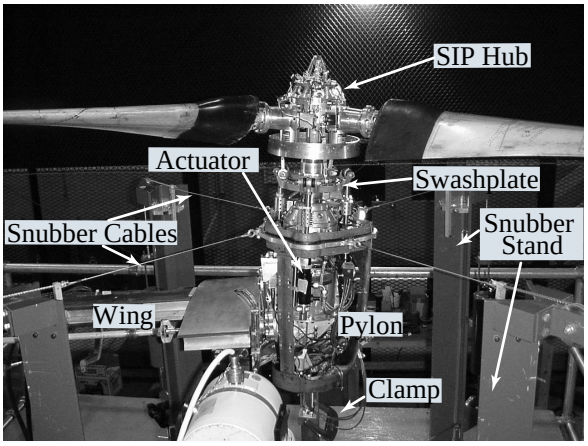

Figure 4: Isolated-rotor hover testing.

electric power source; and a closed-circuit chilled-water system for motor cooling. The model mount was designed to provide stiffness similar to that of the TDT test section side-wall mount so that system frequencies are identical in either the hover cell or the TDT. Testing is monitored in a control room using a closed-circuit camera system and standard televisions. Signal conditioning, data acquisition equipment and the model pilot control console are located side-by-side in the control room. A remote control unit is used to operate the motor-generator set which controls model rotor speed.

Important general features of the WRATS model are listed as follows: an aeroelastically-scaled wing with removable airfoil panels, a dynamically-scaled pylon with a downstop spring tuned to provide elastic mode shapes and frequencies close to those associated with the full-scale conversion actuator (different springs are used for different conversion actuator positions), a gimballed 3-bladed hub with a constant-velocity joint, and a set of aeroelastically-scaled rotor blades. The TDT testing was performed using the baseline stiff-inplane hub, while the hover study was performed with the baseline stiff-inplane hub modified by the addition of lag hinges to provide a soft-inplane rotor configuration. The soft-inplane hub (Fig. 3) is parametrically variable with a set of replaceable coil springs (located behind the lead-lag spring catches) used to tune the lag stiffness, and a set of adjustable hydraulic lead-lag dampers used to tune the lag damping. Gimbal springs are the same for both the stiff-inplane and soft-inplane versions of the hub, and the stiffness of these springs is very small, producing a vacuum rotating flap frequency of about 1.02P. The soft-inplane hub design does not represent an existing full-scale aircraft, rather the current design was developed as a low-cost soft-inplane modification to the existing stiff-inplane gimballed hub (representative of the V-22).

The model is shown configured for hover testing in Fig. 4 surrounded by a snubber system which is used to arrest the model should an instability occur. The snubber is shown activated and the bottom of the pylon is clamped so that isolated rotor testing could be performed (no influence of the wing modes). During normal hover testing there is no clamp and the snubber cables are loosely attached so that the system properties are not effected by the presence of the snubber. Other notable features of the WRATS tiltrotor model shown in Fig. 4 are a hydraulic swashplate and one of the three actuators which are used to position the swashplate. Each actuator is controlled by a servo valve using an attached linear variable displacement transducer (LVDT) for position feedback.

The WRATS wing/pylon dynamic system properties for the helicopter mode and the

Table 1: WRATS fixed-system modal properties.

Helicopter Mode Configuration			**Airplane Mode Configuration**		
Wing Mode Name	Frequency (Hz)	Damping (% crit.)	Wing Mode Name	Frequency (Hz)	Damping (% crit.)
Torsion/Chord	4.56	2.43	Beam	5.83	1.39
Beam	4.97	1.84	Chord	8.67	1.41
Chord/Torsion	12.85	3.67	Torsion	12.02	2.62
Pylon Yaw	16.94	4.03	Pylon Yaw	19.43	4.85

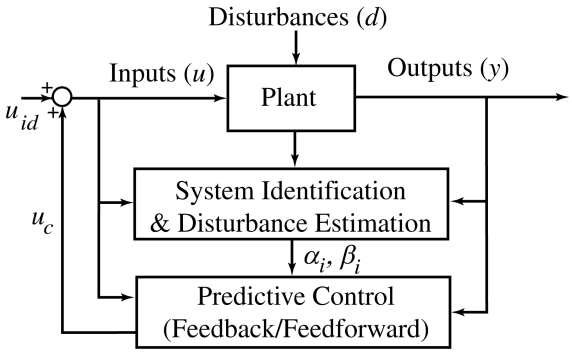

Figure 5: The GPC process.

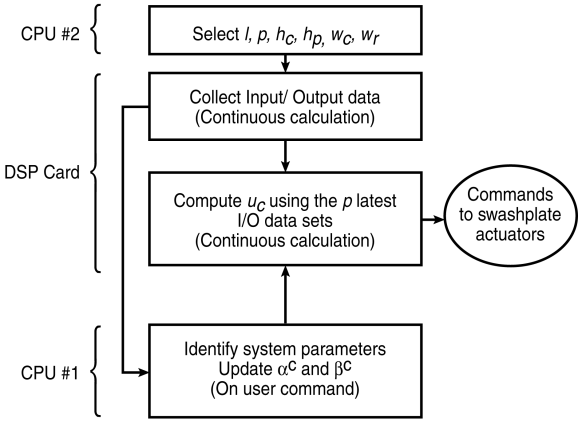

Figure 6: GPC computing tasks.

airplane mode configurations are listed in Table 1. These are the predominant fixed-system (wing) modes, and for each configuration it is the lowest frequency mode which is critical for stability. The wing mode names describe the predominant motion of the wing associated with the mode, and in some cases the motion is highly coupled. The term "Pylon Yaw" is used to describe the 2nd chordwise wing mode which is dominated by the pylon motion in comparison to the motion of the elastic axis.

Typical natural frequencies of the rotor system in cruise (V=100 knots, Ω=742 RPM) are: gimbal flapping 0.85P, first cyclic lag at 1.2P, and collective flapping (coning mode) at about 1.7P. The soft-inplane rotor has similar characteristics except that the first cyclic lag mode is reduced from 1.2P to 0.5P.

3 GENERALIZED PREDICTIVE CONTROL

A novel version of the GPC procedure was developed at NASA Langley Research Center in 1997 for efficient computation and unknown disturbance rejection by Dr. Jer-Nan Juang and his co-workers. Their work has resulted in a suite of MATLAB m-files that have been collected into a Predictive Toolbox that can be used by researchers for GPC studies. A summary of the system identification (SID) and control theory underlying their development is found in Refs. 9 and 10, among others. The key features and equations related to the current implementation of GPC will be discussed only briefly in this section. A more thorough and detailed discussion of GPC as used in these studies is provided in Refs. 11 and 12.

The essential features of the adaptive control process used in the present GPC investigation are depicted in Fig. 5. The system (plant) has r control inputs u, m measured outputs y, and is subject to unknown external disturbances d. Measurement noise is

also present. There are two fundamental steps involved: (1) identification of the system; and (2) use of the identified model to design a controller. A linear input-output model gives the current output variable as a linear combination of past input and output measurements:

$$y(k) = \alpha_1 y(k-1) + \alpha_2 y(k-2) + ... + \alpha_p y(k-p) + \beta_0 u(k) + \beta_1 u(k-1) + ... + \beta_p u(k-p) \quad (1)$$

This equation states that the current output $y(k)$ at time step k may be estimated by using p sets of the previous output and input measurements, $y(k-1)$, ..., $y(k-p)$ and $u(k-1)$, ..., $u(k-p)$; and the current input measurement $u(k)$. The integer p is the order of the model. The coefficient matrices α_i and β_i are referred to as observer Markov parameters and are the quantities to be determined by the SID algorithm.

The one-step ahead output prediction equation (Eqn. 1) is the starting point for deriving the multi-step output prediction equation that is needed for designing a GPC controller. Using Eqn. 1, the output at time step $k+j$ may be written in the form

$$\begin{aligned} y(k+j) \;=\; & \alpha_1^{(j)} y(k-1) + \alpha_2^{(j)} y(k-2) + ... + \alpha_p^{(j)} y(k-p) \\ & + \beta_0 u(k+j) + \beta_0^1 u(k+j-1) + ... + \beta_0^{(j)} u(k) \\ & + \beta_1^{(j)} u(k-1) + \beta_2^{(j)} u(k-2) + ... + \beta_p^{(j)} u(k-p) \end{aligned} \quad (2)$$

This equation shows that the output $y(k+j)$ at time step $k+j$ may be estimated by using p sets of the previous output and input measurements, $y(k-1)$, ..., $y(k-p)$ and $u(k-1)$, ..., $u(k-p)$, and the (unknown) current and future inputs, $u(k)$, $u(k+1)$, ..., $u(k+j)$.

The predictive control law is obtained by minimizing the difference between the predicted controlled response (as computed in Eqn. 2) from a specified target response (which would be zero for stability augmentation) over a user-selected prediction horizon h_p. While not derived here, the resulting control law is given by

$$u_{h_c}(k) = -(T^T R T + Q)^{-1} \times T^T R[-y_T(k) + B u_p(k-p) + A y_p(k-p)] \quad (3)$$

which is valid over the next h_c time steps (h_c is the control horizon and is a user-selectable variable). The coefficient matrices T, B, and A are formed from combinations of the observer Markov parameters α_i and β_i.known from the SID. Q is a weighting matrix used to limit the control effort and stabilize the closed-loop system, and R is used to weight the relative importance of the differences between the target and predicted responses. Also, it is typical in practice for Q to have the same value w_c (control weight) along its diagonal and for R to have the same value w_r (response weight) along its diagonal. Matrix Q must be tuned to ensure a stable closed-loop system, and typically h_c is chosen equal to h_p. However, h_c may be chosen less than h_p resulting in a more stable, but sluggish, regulator. The final and simplified form of the control law is obtained by substituting the expression $\gamma = -(T^T R T + Q)^{-1} \times T^T R$ into Eqn. 3, and then retaining only the first r terms (corresponding to the first future time step):

$$u_c(k) = -\gamma^c y_T(k) + \beta^c u_p(k-p) + \alpha^c y_p(k-p) \quad (4)$$

α^c and β^c are the control law gain matrices and the superscript c is used to denote that only r values are retained from Eqn. 3.

The GPC computer consisted of a 500 MHZ dual processor PC that included a dSPACE

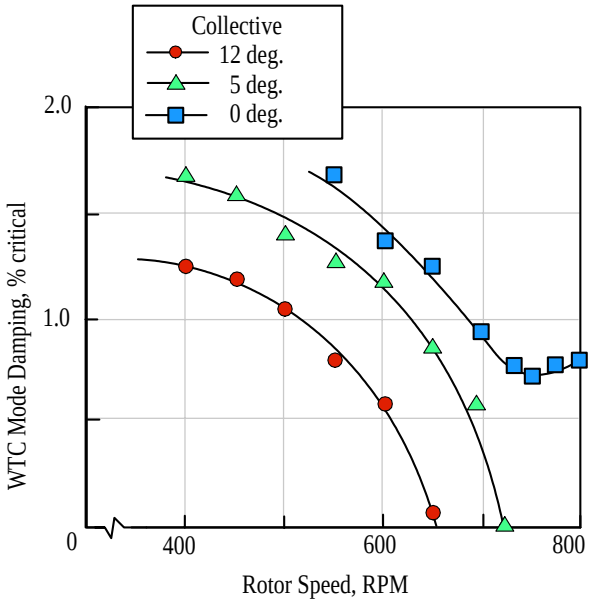

Figure 7: Effect of collective on ground resonance stability in hover, GPC off.

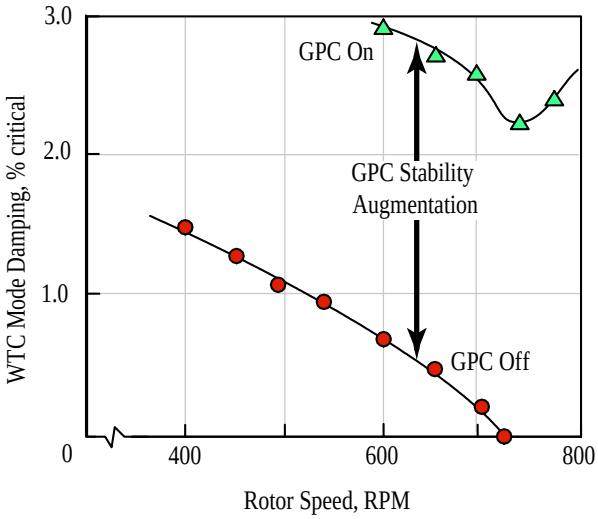

Figure 8: Effect of GPC on ground resonance stability in hover, 8° collective.

DSP1103 add-in card for performing real-time data acquisition and computations. The GPC computational tasks were distributed among these three computing elements in the manner indicated in Fig. 6. The entire process was managed using ControlDesk, dSPACE's graphical user interface (GUI), which was installed on CPU #2. The portion of the GPC algorithm that computes the control gain matrices α^c and β^c is written in MATLAB and runs on CPU #1. The calculation of the control inputs u_c that are sent to the swashplate actuators is made by executable code that is installed on the DSP card. The user specifies appropriate values for the GPC input parameters l (number of time steps used), p, h_p, h_c, w_c, and w_r, and initializes the control gain matrices α^c and β^c to zero. The DSP card continuously collects the r-input and m-output data sets used by the GPC algorithm. On user command, the DSP sends the set of input/output data needed for system identification to CPU #1 where the system identification (SID) computations are performed and the control gain matrices α^c and β^c are computed. The control gain matrices are automatically sent to the DSP which uses the p latest data sets to (continuously) compute the control commands to be sent to the swashplate actuators.

4 HOVER TEST RESULTS (SOFT-INPLANE HUB)

Some of the general characteristics of the ground resonance stability associated with the soft-inplane gimballed tiltrotor model are illustrated in Fig. 7, which shows the variation of the critical wing mode damping with rotor speed for three collective pitch settings. The critical wing mode for this configuration is the wing torsion/chord (WTC) mode. There is a general trend of reduced damping in the WTC mode as rotor speed increases, which is caused mainly by increased coupling between the lag mode and the WTC mode as those associated frequencies coalesce. The plot also indicates that the system behavior is extremely sensitive to collective pitch. This trend is more sensitive than that associated with a typical helicopter rotor system.

Key results of the soft-inplane hover GPC investigation are illustrated in Fig. 8. For the baseline system (GPC off) and a collective pitch setting of 8°, the WTC mode damping is shown to decrease until the model becomes unstable at slightly over 700 RPM. With the

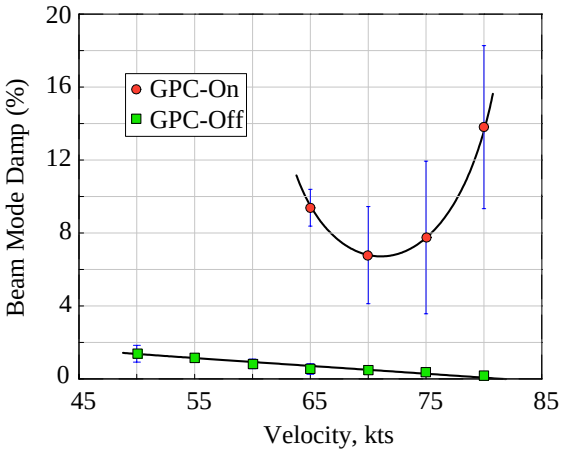

Figure 9: Effect of GPC on wing beam damping, δ_3 = -45°, Ω=888 rpm.

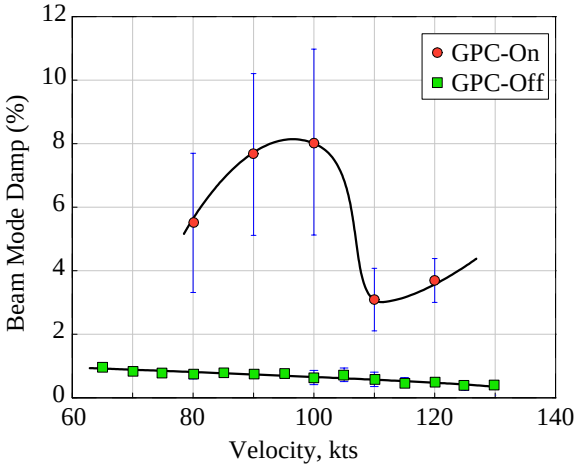

Figure 10: Effect of GPC on wing beam damping, δ_3 = -15°, Ω=888 rpm.

GPC control system activated, a large increase in damping was immediately apparent. The plot shows a consistent increase of about 2% critical damping in the WTC mode, and the system did not become unstable within the rotor design speeds considered. It also should be noted, however, that a great deal of work was performed in obtaining the values for the inputs l, p, and w_c that produced both controller stability and significant damping increases for the model. It was not uncommon during the process of tuning the controller to develop a control instability and then have to shut the control system down and/or snub the model.

5 WIND-TUNNEL TEST RESULTS (STIFF-INPLANE HUB)

The GPC-based active control system was found highly effective in increasing the stability (damping) of the critical wing mode for all of the configurations of the model tested. In particular, GPC was able to consistently yield a closed-loop system in which the critical wing mode had a minimum of about 3% modal damping over the range of test conditions investigated, without visible degradation of the damping in the other modes. The GPC algorithm was robust with respect to its performance in the tracking of rapid changes in both the rotor speed and the tunnel air-speed. System identification done at a low-speed flight condition was generally sufficient for a wide range of rotor speeds and tunnel velocities.

An indication of the effectiveness of the GPC-based active control system in increasing the stability (damping) of the critical wing beam mode of the model is given in Figs. 9 and 10. The figures show a comparison of the measured open-loop and closed-loop wing beam mode damping versus airspeed for blade pitch-flap coupling (δ_3 angle) values of $-45°$ and $-15°$, respectively. The mean and standard deviation of the five (or more) values of damping that were measured at each airspeed were determined. The mean values of damping are indicated by the symbols, and the vertical lines (error bars) indicate the standard deviations about these mean values. The plotted curves are the result of a spline fit applied to the mean values. As can be seen with GPC turned on, the wing beam mode damping is considerably higher than with GPC off over the entire range of tunnel airspeeds tested. It should be noted that with GPC on it was often difficult to estimate the damping from the free-decay responses after termination of the forced excitation because the large damping levels resulted in very few cycles of motion (sometimes as few

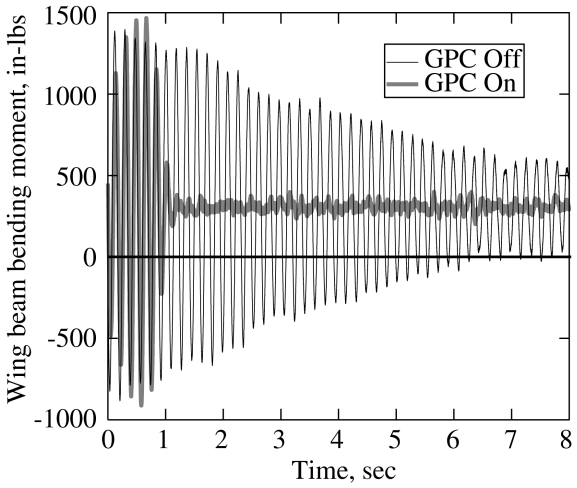

Figure 11: Effect of GPC on wing response, 75 knots, $\delta_3 = -45°$.

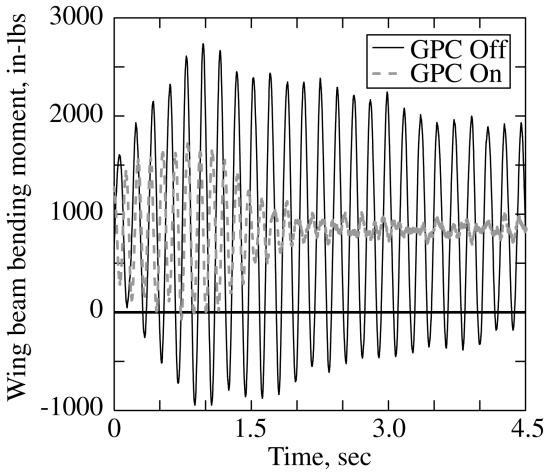

Figure 12: Effect of GPC on wing response, 120 knots, $\delta_3 = -15°$.

as one or two) being available for the damping calculations. This is the reason for the large standard deviation in the measured values of the closed-loop damping. In contrast, because the open-loop damping of the wing beam mode is small, the standard deviation of the measured damping is correspondingly very small. It should also be noted that the effectiveness of GPC was such that it tried to quell the imposed stick-stir excitation, thus requiring considerable amplitude of excitation.

The measured time histories of the wing beam bending moments during and after a typical stick-stir excitation with GPC on and off are shown in Figs. 11 and 12. Fig. 11 corresponds to the 75 knot airspeed of Fig. 9 and Fig. 12 corresponds to the 120 knot airspeed of Fig. 10. The closed-loop time histories clearly illustrate the effectiveness of the GPC-based active control system to rapidly reduce the response. Similar results were obtained at the other airspeeds.

Another example of the effectiveness of GPC is given in Fig. 13, which shows a time history of the wing beam bending moment while repeatedly cycling GPC on and off. The data correspond to the case of Fig. 10 at 120 knots. These results indicate that the GPC algorithm is robust with respect to on/off cycling and that reinitialization of the control system occurs very quickly. An indication of the swashplate pitch angles that are associated with the GPC commanded actuator inputs is given in Fig. 14. The figure shows the time history of the longitudinal and lateral cyclic pitch angles from a time near the end of a stick-stir excitation to a time well within the steady-state condition. The results correspond to the 120-knot airspeed condition shown in Fig. 10. The steady-state oscillatory cyclic pitch angles are modest, indicating that implementation of GPC probably has a noticeable but not significant effect on the control system loads (not measured directly in this test).

6 CONCLUSIONS

Researchers from Langley Research Center (LaRC) and Bell Helicopter-Textron, Inc. (BHTI) have completed two experimental studies of active stability augmentation on the Wing and Rotor Aeroelastic Testing System (WRATS), a 1/5-size aeroelastic semi-span model based on the V-22, using an adaptive, Multi-Input Multi-Output (MIMO), Generalized Predictive Controller (GPC) algorithm, combined with an active swashplate control system. The investigations considered a soft-inplane gimballed hub subject to

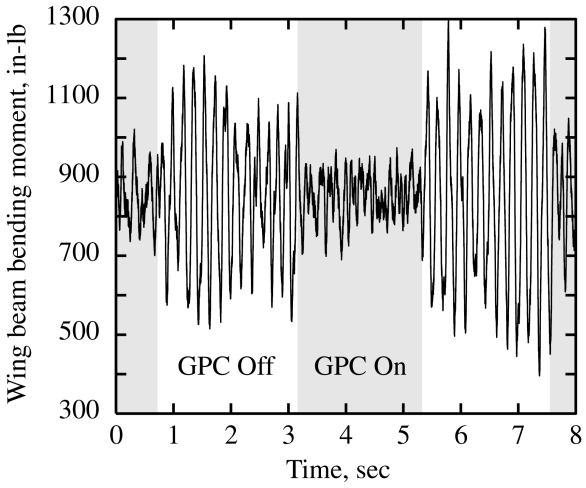

Figure 13: Wing response with GPC cycled on and off, 120 knots, $\delta_3 = -15°$.

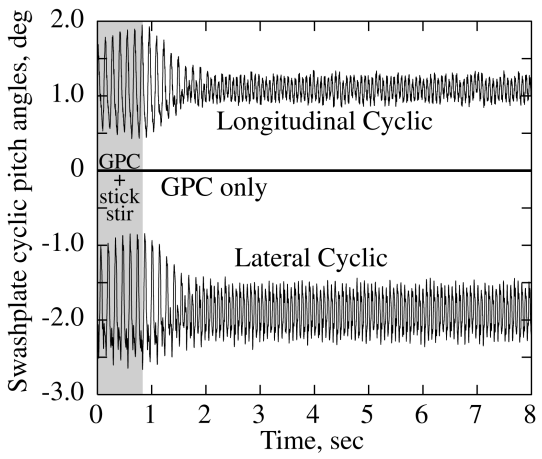

Figure 14: Closed-loop swashplate cyclic pitch, 120 knots, $\delta_3 = -15°$.

ground resonance conditions in hover (October 1999), and a stiff-inplane gimballed hub subject to whirl-flutter conditions in airplane mode (April 2000).

With respect to ground resonance behavior, the soft-inplane rotor system tested in hover showed an expected trend of decreasing damping in the critical wing mode as rotor speed was increased, in most cases leading to an instability. GPC with an active swashplate proved to be highly effective at increasing damping and eliminating the ground resonance induced instabilities, and the controller was robust with respect to changes in rotor speed.

In the wind-tunnel investigation, closed-loop stability of the model resulting from GPC inputs computed using feedback from wing-root strain gages was measured over a range of steady tunnel airspeeds for a single rotor rotational speed and two values of kinematic pitch-flap coupling. Performance of the system was also assessed in transient conditions by rapidly changing tunnel velocity and rotor speed about a nominal operating condition. Based on the results obtained in this investigation, the following conclusions are indicated:

1. The GPC algorithm employed was highly effective in increasing the stability (damping) in the critical wing mode of the model tested.

2. The GPC algorithm employed was also robust with respect to rapid changes in both the rotor speed and the airspeed, either singly or in combination.

3. All system identification and control law computations were done on-line, permitting rapid adaptation to changing conditions.

4. The swashplate angles required were modest, generally less than 0.4 degrees.

These results from the wind-tunnel and the hover ground resonance test suggest that a GPC-based active control system is a viable candidate for stability augmentation in advanced tiltrotor systems. Additional wind-tunnel and hover tests of the WRATS model are planned to evaluate the GPC methodology over a broader range of operating conditions using a new semi-articulated soft-inplane hub design.

7 REFERENCES

1. Agnihotri, A., Schuessler, W., and Marr, R.: "V-22 Aerodynamic Loads Analysis and Development of Loads Alleviation Flight Control System." 45th Annual forum of the American Helicopter Society, Boston, Massachusetts, May 1989.

2. Alexander, H.R., Hengen, L.H., and Weiberg, J.A.: "Aeroelastic-Stability Characteristics of a V/STOL Tilt-Rotor Aircraft with Hingeless Blades: Correlation of Analysis and Test." 30th Annual Forum of the American Helicopter Society, May 1974.

3. Magee, J.P., Alexander, H.R., Gillmore, K.B., Richardson, D.A., and Peck, W.B..: "Wind Tunnel Tests of a Full Scale Hingeless Prop/Rotor Design for the Boeing Model 222 Tiltrotor Aircraft." Report No. D222-10059-1, Contract NAS2-6505, April 1973.

4. Johnson, W.: "Dynamics of Tilting Proprotor Aircraft in Cruise Flight." NASA TN D-7677, May 1974.

5. Alexander, H.R., Eason, W., Gillmore, KI., Morris, J., and Spittle, R.: "V/STOL Tilt Rotor Aircraft Study. Volume 7: Tilt Rotor Flight Control Program Feedback Studies. NASA CR-114600, March 1973.

6. Nasu, K.: "Tilt-Rotor Flutter Control in Cruise Flight." NASA TM 88315, December 1986.

7. Van Aken, J. M.: "Alleviation of Whirl-Flutter on Tilt-Rotor Aircraft Using Active Control." Proceedings of the 47th Annual Forum of the American Helicopter Society, Phoenix, AZ, May 6-8, 1991, pp. 1321-1344.

8. Vorwald, J. G., and Chopra, I.: "Stabilizing Pylon Whirl Flutter on a Tilt-Rotor Aircraft." Presented at the 32nd AIAA/ASME/ASCE/AHS/ASC Structures, Structural Dynamics, and Materials Conference, Baltimore, MD, April 8-10, 1991 (Paper AIAA 91-1259-CP).

9. Juang, J.-N.: *Applied System Identification*. Prentice Hall, Inc., Englewood Cliffs, New Jersey 07632, 1994, ISBN 0-13-079211-X.

10. Juang, J.-N. and Eure, K. W.: "Predictive Feedback and Feedforward Control for Systems with Unknown Disturbances." NASA TM-1998-208744, December 1998.

11. Nixon, M.W., *et.al.*, "Aeroelastic Stability of a Soft-Inplane Gimballed Tiltrotor Model in Hover." Presented at the 42nd AIAA/ASME/ASCE/AHS/ASC Structures, Structural Dynamics, and Materials Conference, Seattle, Washington, April 16-19, 2001.

12. Kvaternik, *et. al.*, "An Experimental Evaluation of Generalized Predictive Control for Tiltrotor Aeroelastic Stability Augmentation in Airplane Mode of Flight." Presented at the American Helicopter Society 57th Annual Forum, Washington, D.C., May 9-11, 2001.